



LAWRENCE  
LIVERMORE  
NATIONAL  
LABORATORY

# Particle Size-Dependent Photoelectron Plasmon Loss Features In Deposited Germanium Nanocrystals

C. Bostedt, T. Willey, L. Terminello, T. van Buuren

March 9, 2012

Electrochemical Society  
Seattle, WA, United States  
June 8, 2012 through June 12, 2012

## **Disclaimer**

---

This document was prepared as an account of work sponsored by an agency of the United States government. Neither the United States government nor Lawrence Livermore National Security, LLC, nor any of their employees makes any warranty, expressed or implied, or assumes any legal liability or responsibility for the accuracy, completeness, or usefulness of any information, apparatus, product, or process disclosed, or represents that its use would not infringe privately owned rights. Reference herein to any specific commercial product, process, or service by trade name, trademark, manufacturer, or otherwise does not necessarily constitute or imply its endorsement, recommendation, or favoring by the United States government or Lawrence Livermore National Security, LLC. The views and opinions of authors expressed herein do not necessarily state or reflect those of the United States government or Lawrence Livermore National Security, LLC, and shall not be used for advertising or product endorsement purposes.

## Particle Size-Dependent Photoelectron Plasmon Loss Features In Deposited Germanium Nanocrystals

C. Bostedt<sup>a</sup>, T. M. Willey<sup>b</sup>, N. Franco<sup>b</sup>, L. J. Terminello<sup>c</sup> and T. van Buuren<sup>b</sup>

a) Stanford Linear Accelerator Ctr, Natl Accelerator Lab, Stanford, CA 94309, USA

b) Lawrence Livermore National Laboratory, 7000 East Ave, Livermore, CA 94550, USA

c) Pacific Northwest National Laboratory, 902 Battelle Boulevard, Richland, WA 99352, USA

The plasmon loss features of deposited and well-characterized germanium nanocrystals with average sizes of 3.5 and 4.5~nm, respectively, are investigated with photoelectron spectroscopy at the Ge~3d core level. We observe a particle size dependence of the surface plasmon amplitude with respect to the bulk plasmon consistent with the changing surface-to-bulk atom ratio. Additionally, the nanocrystal surface plasmons are redshifted with respect to a bulk reference by up to 0.4~eV for 3.5~nm particles. For the bulk plasmons no significant size dependent energy shifts can be observed for nanoparticle sizes down to 3.5~nm.

The plasmon loss feature in group IV semiconductor nanocrystals has recently sparked significant interest and some controversy. Transmission electron microscope studies on Si nanoclusters and x-ray photoelectron spectroscopy studies on ultrathin Si films, and porous Si found large blueshifts in the plasmon energy from 0.2 eV for 10 nm particles up to 2.3 eV for 2 nm structures which were attributed to quantum confinement effects. (1-4) This reported increase in the plasmon energy is much larger than the quantum confinement effects found in the bandgap of Si nanocrystals. (5) Transmission electron microscope energy loss spectrometer (STEM-ELS) has been used to study plasmons in Ge nanowires. They found that the bulk plasmon energy increases with decreasing diameter for nanowires narrower than 24 nm. (4) In contrast to the plasmon energy measurements, calculations of the electron energy loss spectra in silicon nanostructures predicted that the plasmon energy did not show any size dependence for particles larger than ~ 50 atoms corresponding to approximately 1 nm particle size. (6) These calculations lead to different conclusions in a further experimental study. Here, a blueshift of the plasmon energy in Ge nanocluster films vanished upon annealing that was related to a phase transition in the particles.(7) Surprisingly, none of the experimental data above shows clear surface plasmon loss features. (1-4) Surface plasmon intensities are expected to increase with decreasing particle size due to the rapidly changing surface-to-bulk atom ratio in nanostructures. To shed more light on both controversies, the plasmon energy and the surface-to-bulk ratio, we explored the plasmon loss features in a very well characterized system of germanium nanocrystals with synchrotron radiation based photoelectron spectroscopy (PES) in a more surface sensitive energy regime. Germanium was chosen as cluster material because Ge nanocrystals can be synthesized in a very controlled manner, and the nanoparticle structure was carefully analyzed with various approaches.(8-10) Also, germanium nanocrystals were predicted to exhibit equal or greater quantum confinement effects than similarly-sized silicon nanocrystals what was experimentally

confirmed in the empty states. (11-14) The reported experiments will yield a valuable input from a very well defined system for further discussion and modeling of plasmon loss features in semiconductor nanostructures.

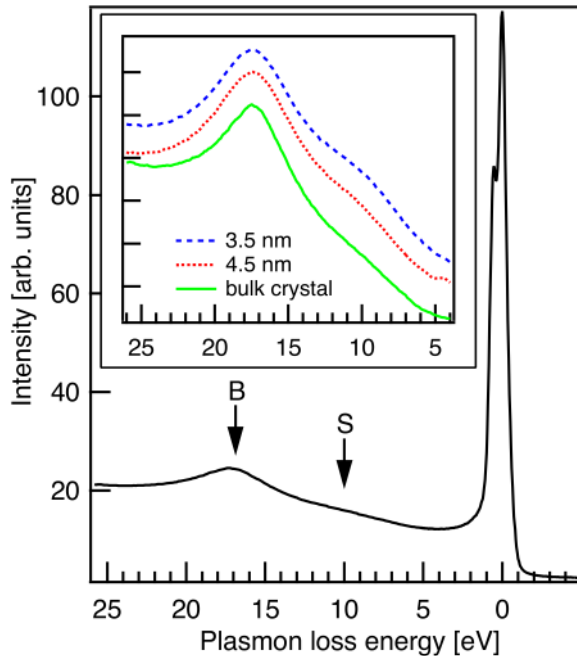


**Figure 1:** Ge 3d core level with corresponding plasmon loss feature for a bulk crystal reference. In the inset the Plasmon data for a bulk reference, 4.5 and 3.5 nm nanocrystal sample is shown on a smaller scale.

4.5 nm average size were prepared. The particle sizes exhibit a narrow distribution of 20% FWHM.(8) As substrates carefully outgassed, native oxide terminated silicon wafers were used. Multiple monolayers of nanocrystals were deposited to obtain a complete coverage of the substrate as monitored by Si 2p core level photoemission. The resulting films consisted of individual nanocrystals on top of each other as evidenced by atomic force microscopy.(8) To avoid oxidation of the sample from residual gas, the base pressure was kept on the order of  $10^{-9}$  Torr in the synthesis chamber and  $10^{-10}$  Torr in the detector chamber. To measure the loss features, synchrotron-radiation based PES was performed at the Ge 3d core level. The experiments were carried out at the high-flux, high-resolution undulator beamline 8.0 at the Advanced Light Source (ALS) at Lawrence Berkeley National Laboratory.(14) For photoelectron detection the ellipsoidal mirror analyzer endstation was used.(16) The joint resolution of the beamline and detector was estimated to be 0.3 – 0.4 eV. The incoming photon flux was measured with a highly transmissive (> 90%) gold grid and all spectra were normalized with respect to this flux. For the photoemission experiments a photon energy of  $h\nu = 200$  eV was chosen. In Fig. 1 the Ge 3d core level with the corresponding surface (S) and bulk (B) plasmon for a bulk reference is shown. The inset in Fig. 1 contains the as-taken Plasmon data for the bulk reference plus the 4.5 and 3.5 nm nanocrystal samples on an expanded y-axis. For ease of reference the x-axis is scaled with respect to the Ge 3d core level, i.e., plasmon energy. For all three samples the plasmon region is dominated by the secondary electron background but some

The nanocrystals were synthesized in a gas-aggregation type source and subsequently deposited in situ at the beamline.(8) In brief, germanium is evaporated into a He buffer gas atmosphere and nanoclusters condense out of the supersaturated vapor. Structural analysis of nanoparticles 4–5 nm in size showed the particles to be in the bulk-like cubic (diamond) phase.(8) Early photoemission experiments revealed a distribution of Ge 3d surface core-level shifts indicating a disordered nanocrystal surface.(8) A recent combined study of photoelectron spectroscopy and first principles electronic structure calculations identified the structure for particles down to 2 nm as distorted diamond lattice core with a reconstructed surface layer.(10) For the current plasmon measurements two nanocrystal depositions with 3.5 and

important trends can be already identified in the as-taken data. The surface plasmon intensity is increasing with respect to the bulk plasmon with decreasing particle size in agreement with the increasing surface-to-bulk atom ratio. Such a clear increase in the surface plasmon intensity has not yet been reported in the literature. Compared to the bulk reference, the plasmon features of the nanocrystals are broadened. For further analysis of the plasmon excitations, a modeled secondary electron background is subtracted from the as-measured spectra. After comparing the results of various background types, a Shirley-type background is chosen. In this secondary electron background model the loss function is approximated by a function with magnitude at each point proportional to the spectrum area at lower binding energy. The background corrected data for the nanocrystal samples and the bulk reference is shown in Fig. 2. For better comparability the three curves are scaled to the same overall peak height. In the background corrected data the bulk and surface plasmon features can be clearly distinguished and the strongly increasing intensity of the surface plasmon with respect to the bulk plasmon becomes obvious. Also, the nanocrystal Plasmon excitations are significantly broadened compared to the bulk crystal reference. The plasmon loss features can be well fitted with a dominant first order bulk and surface contribution plus a second order surface peak. The second order bulk distribution is outside the considered energy window.

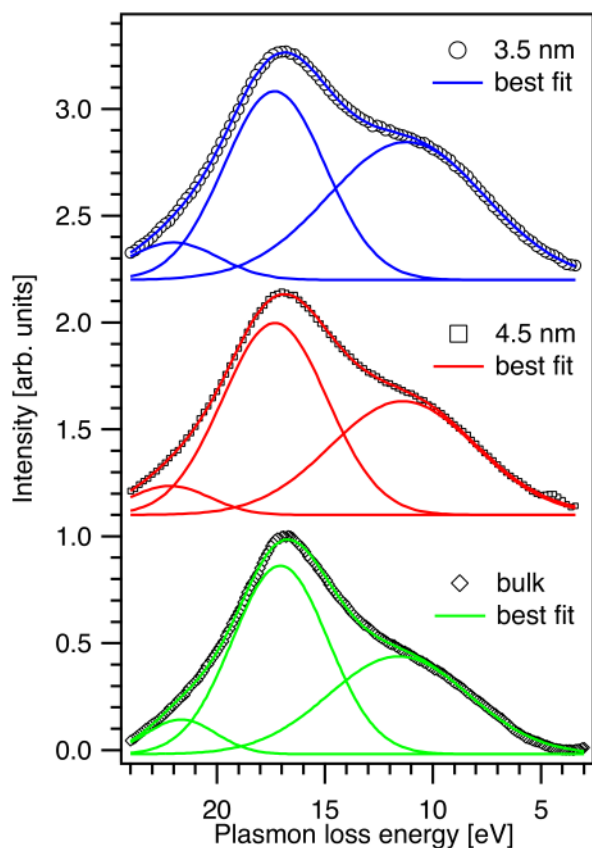


**Figure 2:** Background subtracted data and best fits for the secondary electron background corrected data from Fig. 1.

The nanocrystal surface and bulk plasmons are best described with Gaussian line shapes indicating typical broadening effects for nanocrystalline samples such as their non-perfect crystal structure and size distribution. Similar broadening effects were observed in photoelectron spectroscopy of Ge nanocrystals and band edge investigation of Si<sub>4</sub> and Ge<sub>13</sub> nanoparticles. (9) The fitting results for the plasmon intensities are summarized in table I, the results for their energies are summarized in table II. The peak intensities (table I) show a clear increase in the surface-plasmon to bulk-plasmon amplitude ratio from 0.51 for the bulk reference to 0.59 for 4.5 nm particles and up to 0.72 for 3.5 nm particles. Due to broadening of the resonances with decreasing size (compare table II), shown. The inset in Fig. 1 contains the as-taken plasmon data for the bulk reference plus the 4.5 and 3.5 nm nanocrystal samples on an expanded y-axis. For ease of reference the x-axis is scaled with respect to the Ge

3d core level, i.e., plasmon energy. For all three samples the plasmon region is dominated by the secondary electron background but some important trends can be already identified in the as-taken data. The surface plasmon intensity is increasing with respect to the bulk plasmon with decreasing particle size in agreement with the increasing surface-to-bulk atom ratio. Such a clear increase in the surface plasmon intensity has not yet been reported in the literature. Compared to the bulk reference, the plasmon features of the nanocrystals are broadened.

For further analysis of the plasmon excitations, a modeled secondary electron background is subtracted from the as-measured spectra. After comparing the results of various background types, a Shirley-type background is chosen. In this secondary electron background model the loss function is approximated by a function with magnitude at each point proportional to the spectrum area at lower binding energy. The background corrected data for the nanocrystal samples and the bulk reference is shown in Fig. 2. For better comparability the three curves are scaled to the same overall peak height. In the background corrected data the bulk and surface plasmon features can be clearly distinguished and the strongly increasing intensity of the surface plasmon with respect to the bulk plasmon becomes obvious. Also, the nanocrystal plasmon excitations are significantly

**TABLE I.**

	<b>Peak height (area) Surface</b>	<b>Peak height (area) Bulk</b>	<b>Peak height (area) Ratio</b>
Bulk	0.45 (3.7)	0.88 (4.9)	0.51 (0.750)
4.5 nm	0.53 (4.5)	0.89 (5.4)	0.59 (0.83)
3.5nm	0.64 (5.9)	0.88 (5.20)	0.72 (1.13)

TABLE I: Peak heights and area (in brackets) for the plasmon excitations of a bulk reference and two nanocrystal samples from Fig. 2 .

**TABLE II.**

	<b>Plasmon Energy (width) [eV] Surface</b>	<b>Plasmon Energy (width) [eV] Bulk</b>
Bulk	11.6 (3.2)	17.1 (2.2)
4.5 nm	11.4 (3.4)	17.3 (2.4)
3.5nm	11.2 (3.6)	17.3 (2.3)

TABLE II: Plasmon energies and width (in brackets) for a bulk reference and two nanocrystal samples determined from Fig. 2.

broadened compared to the bulk crystal reference. The plasmon loss features can be well fitted with a dominant first order bulk and surface contribution plus a second order surface peak. The second order bulk distribution is outside the considered energy window. The nanocrystal surface and bulk plasmons are best described with Gaussian line shapes indicating typical broadening effects for nanocrystalline samples such as their non-perfect crystal structure and size distribution. Similar broadening effects were observed in photoelectron spectroscopy of Ge nanocrystals and band edge investigation of Si and Ge nanoparticles. (5,9,14) The fitting results for the plasmon intensities are summarized in table I, the results for their energies are summarized in table II. The peak intensities (table I) show a clear increase in the surface-plasmon to bulk-plasmon amplitude ratio from 0.51 for the bulk reference to 0.59 for 4.5 nm

particles and up to 0.72 for 3.5 nm particles. Due to broadening of the resonances with decreasing size (compare table II), especially for the nanoparticle surface plasmon, the effect is even more drastic when the peak areas are compared. Here the surface to bulk ratio increases from 0.75 for the bulk reference up to 1.13 for the 3.5 nm particle. The observation of size dependent plasmon intensities show that the nanoparticles exhibit even for collective phenomena distinct surface and bulk contributions. However, neither the fitted peak amplitude nor the peak area surface-to-bulk ratio can directly reflect the fraction of surface atoms to bulk atoms in the nanocrystal. The surface-plasmon to bulk-plasmon intensity is distorted by the limited sampling depth of the photoemission technique. For the present surface sensitive experiment with electron kinetic energies of  $\sim 160$  eV the electron escape depth is only  $\sim 0.7$  nm. (17) Considering that the principal energy loss in the core level photoemission process is the plasmon excitation, the sampling depth for the first excited plasmon can be roughly approximated to twice the escape depth, i.e.,  $\sim 1.4$  nm. Therefore the obtained information in the current experiments does not reflect the overall particle but only the particle top cap. The limited electron escape depth, or in other words the high surface sensitivity, also explains the observed high surface-plasmon to bulk-plasmon ratio for the bulk reference of 0.51 (peak area 0.75) compared to 0.59 (peak area 0.83) for the 4.5 nm particle. Also in the case of the bulk reference, a surface layer and not the semi-infinite crystal is probed.

In addition to the changing intensity ratios the fits reveal interesting results on the plasmon energies. The bulk-plasmon of the nanoparticle samples is blue shifted by 0.2 eV with respect to the bulk reference and slightly broadened by 0.2 (0.1) eV for the 4.5 (3.5) nm sample. The very small and not size dependent blue shift of the nanocrystal bulk plasmon is in contrast to earlier investigations on silicon nanostructures for which strong plasmon energy blue shifts from 0.2 eV for 10 nm particles up to 2.3 eV for 2 nm structures were reported. These blue shifts were attributed to quantum confinement effects. (1–4) Quantum confinement effects in germanium are expected to be similar to or greater than in silicon and therefore comparisons between both systems are substantiated. While there are discrepancies between the present and the earlier experimental studies, the present results agree with theoretical predictions that there is no bulk plasmon energy size-dependence in silicon nanostructures larger than 50 atoms, i.e., about 1 nm.(5) We note that our results are consistent

Furthermore, the present results agree with investigations about quantum confinement effects at the band edges of silicon and germanium nanocrystals. (5,14) In those experiments no significant quantum shifts could be observed for particles above 3 to 4 nm in size. From the present experimental results and the comparison to theoretical predictions it must be concluded that the bulk plasmon energies in nanoclusters do not exhibit any significant quantum confinement effects for particle sizes down to 3.5 nm. For completeness it shall be pointed out that the present and previous samples are films of nanocrystals whereas the electronic structure measurements were performed on individual particles. (1-5,7,14) Conduction band edge measurements on both systems, films and individual particles, show that the particle electronic structure can be affected by contact between the particles.(18)

In contrast to the bulk plasmon energies, the surface plasmons exhibit a clear size dependence. The nanocrystal surface plasmons are red shifted by 0.2 eV (0.4 eV) for the 4.5 nm (3.5 nm) sample with respect to the bulk crystal reference. Further, they exhibit an increasing line broadening up to 0.4 eV with decreasing particle size. The observed red shift of the surface plasmon is in contradiction to the quantum confinement interpretation of the bulk plasmon in earlier studies.(1–3) It should be mentioned that the surface plasmon feature reported here could

not be resolved previously. Compared to these earlier investigations the sample preparation and characterization have been greatly improved, allowing more accurate fitting of the plasmon intensities and energies. The unexpected observation of red shifted surface plasmons can be attributed to the particle structure, in particular the particle surface shell. The nanocrystals exhibit a heavily reconstructed surface with a variation of bond angles and length. (10) This leads to significant alterations of the charge density in the surface area with the effect being larger for smaller particles. Theoretically, Delerue et. al show for small silicon clusters that multiple surface plasmon resonances exist between 5 and 16 eV loss energy (for silicon the bulk plasmon energy is around 18 eV) depending on the size and thus geometry.(6) Experimentally, it is well known that small metal clusters can exhibit multiple plasmon excitations depending on the size and shape of the particles due to different polarizabilities.(19) Similarly, the reconstructed surface shell of semiconductor nanoparticles with altered charge densities and broken symmetries will lead to a distribution of Plasmon excitations which can explain the observed broadening and red shift of the surface plasmon loss peak.

In conclusion we have investigated the Ge 3d Plasmon loss features of well characterized Ge nanocrystal depositions of 4.5 and 3.5 nm in size. We find that the surface plasmon intensity is strongly increasing with respect to the bulk plasmon for decreasing nanoparticle sizes, consistent with the increasing surface-to-bulk atom ratio. For the bulk plasmon energies of the nanoclusters down to 3.5 nm no significant quantum confinement shifts could be measured indicating that if such effects exist they only occur in the smallest nanoparticles. Additionally we observe a decrease in the surface plasmon energies of up to 0.4 eV which is attributed to the changing surface geometry for nanocrystals.

### Acknowledgments

The Advanced Light Source is supported by the U.S. Department of Energy under Contract No. DE-AC03-76SF00098 at Lawrence Berkeley National Laboratory. This work was partially supported by the Office of Basic Energy Sciences (OBES), Materials Science Division (MSD), under the auspices of the U.S. DOE by LLNL under Contract DE-AC52-07NA27344.

### References

1. M. Mitome, Y. Yamazaki, H. Takagi, and T. Nakagiri, *J. Appl. Phys.* **72**, 812 (1992).
2. N. Dibiasi, G. Gabetta, A. Lumachi, M. Scagliotti, and F. Parmigiani, *Appl. Phys. Lett.* **67**, 2491 (1995).
3. N. Mannella, G. Gabetta, and F. Parmigiani, *Appl. Phys. Lett.* **79**, 4432 (2001).
4. T. Hanrath, B.A. Korgel, *Nano Lett.*, **4**, 1455-1461 (2004).
5. T. van Buuren, L. N. Dinh, L. L. Chase, W. J. Siekhaus, and L. J. Terminello, *Phys. Rev. Lett.* **80**, 3803 (1998).
6. C. Delerue, G. Lannoo, and G. Allan, *Phys. Rev. B* **56**, 15306 (1997).
7. S. Sato, S. Nozaki, and H. Morisaki, *Thin Solid films* **343-344**, 481 (1999).
8. C. Bostedt, T. van Buuren, J. M. Plitzko, T. Moller, and L. J. Terminello, *J. Phys. Condens. Matter* **15**, 1017 (2003).
8. C. Bostedt, T. van Buuren, T. M. Willey, N. Franco, T. Moller, and L. J. Terminello, *J. Electron Spectrosc. Relat. Phenom.* **126**, 117 (2002).

9. A. J. Williamson, C. Bostedt, T. van Buuren, T. M. Willey, L. J. Terminello, G. Galli, and L. Pizzagalli, *Nano Lett.* **4**, 1041 (2004).
10. F. A. Reboredo and A. Zunger, *Phys. Rev. B* **62**, 2275 (2000).
11. N. A. Hill, S. Pokrant, and A. J. Hill, *J. Phys. Chem. B* **103**, 3156 (1999).
12. T. Takagahara and K. Takeda, *Phys. Rev. B* **46**, 15578 (1992).
13. C. Bostedt, T. van Buuren, T. M. Willey, N. Franco, L. J. Terminello, C. Heske, and T. Moller, *Appl. Phys. Lett.* **84**, 4056 (2004).
14. J. J. Jia, T. A. Calcott, J. Yurkas, A. W. Ellis, F. J. Himpsel, M. G. Samant, J. Stohr, D. L. Ederer, J. A. Carlisle, E. A. Hudson, et al., *Rev. Sci. Instrum.* **66**, 1394 (1995).
15. D. E. Eastman, J. J. Donelon, N. C. Hien, and F. J. Himpsel, *Nucl. Instrum. Meth.* **172**, 327 (1980).
16. M. Cardona and L. Ley, *Photoemission in Solids I: General principles*, vol. 26 of *Topics in Applied Physics* (Springer-Verlag, 1978).
17. C. Bostedt, T. van Buuren, T. M. Willey, and Terminello, *Appl. Phys. Lett.* **85**, 5334 (2004).
18. W. Eberhardt, *Surf. Sci.* **500**, 242 (2002)